Phys. Status Solidi B **248**, No. 1, 52–59 (2011) / **DOI** 10.1002/pssb.201083980

physica status solidi b
www.pss-b.com
basic solid state physics

Modelling of hexagonal honeycombs exhibiting zero Poisson's ratio

Daphne Attard and Joseph N. Grima*

Faculty of Science, University of Malta, Msida MSD 2080, Malta

Received 10 June 2010, revised 27 July 2010, accepted 30 July 2010
Published online 24 September 2010

Keywords honeycombs, modelling, mechanical properties, zero Poisson's ratio, auxetic, negative Poisson's ratio

* Corresponding author: e-mail joseph.grima@um.edu.mt, Phone: +356 2340 2274 / +356 7904 9865, Fax: +356 2133 0400

A detailed analytical model for novel hexagonal honeycomb structures which are composed of alternate layers of re-entrant and non re-entrant features is presented. It is shown that deformation from hinging, flexure and/or stretching of the cell walls can lead to zero Poisson's ratios, a property which is highly desirable in niche applications.

1 Introduction In recent years there have been several studies on two-dimensional honeycombs [1–31] with particular attention being paid to honeycombs based on hexagonal cells such as the ones illustrated in Fig. 1. Despite being very simple, such honeycombs are used in various practical applications, for example, as the matrix in sandwich panels where they are sandwiched between two hard skins to produce lightweight high-strength composites which are then used in the manufacture of products ranging from aircrafts to domestic internal doors.

Of particular significance is the work which examines the mechanical properties of such honeycombs. In particular, Gibson and Ashby [1, 2] have derived equations for the in-plane properties of the hexagonal honeycomb systems illustrated in Fig. 1a and b deforming through flexure of the cell walls and show that the in-plane Poisson's ratios ν_{ij} and Young's moduli E_i for loading in the Ox_i directions are given by:

$$\nu_{21} = \nu_{12}^{-1} = \frac{[h/l + \sin(\theta)]\sin(\theta)}{\cos^2(\theta)},$$

$$E_1 = E_s\left(\frac{t}{l}\right)^3 \frac{\cos(\theta)}{[h/l + \sin(\theta)]\sin^2(\theta)}$$

$$E_2 = E_s\left(\frac{t}{l}\right)^3 \frac{h/l + \sin(\theta)}{\cos^3(\theta)}.$$

where as illustrated in Fig. 1, l is the length of the inclined ribs, h the length of the vertical ribs, t the thickness of the ribs, θ is the angle the inclined ribs make with the horizontal (positive for conventional honeycombs and negative for re-entrant ones) whilst E_s is the intrinsic Young's moduli of the honeycombs. This derivation clearly showed that when θ is negative, the Poisson's ratio is also negative. This was one of the major milestones in the field of such materials (also known as auxetic materials [3, 4, 16–66]) which have various practical applications [13, 35, 43, 44, 67–75]. A significant amount of work on auxetics has been directed towards the analysis of various re-entrant honeycombs [3, 4, 24–33] (*i.e.* honeycombs where θ is negative) which were predicted to exhibit a negative Poisson's ratio if they deform through flexure.

In particular, the models by Gibson and Ashby were further extended by Evans et al. in their seminal papers which consider a more generalized model which can deform through simultaneous flexure, hinging and/or stretching of the cell walls [3, 4]. Such analysis had shown that re-entrant honeycombs will exhibit negative Poisson's ratio if they deform through hinging and/or flexing of the cell walls but will exhibit conventional positive Poisson's ratios if the re-entrant honeycombs deform through stretching. Conversely, non re-entrant honeycombs were shown to exhibit positive Poisson's ratio if they deform through hinging and/or flexing of the cell walls but will exhibit auxetic behaviour if they deform though stretching.

The equations for the mechanical properties of these honeycombs suggest that for particular variable combinations, the honeycombs can also exhibit the property of zero Poisson's ratio. In particular, honeycombs with $\theta = 0$ will exhibit zero Poisson's ratio when loaded in the Ox_1 direction if they deform through stretching. Similarly zero Poisson's ratio behaviour is observed for loading in the Ox_2 direction if

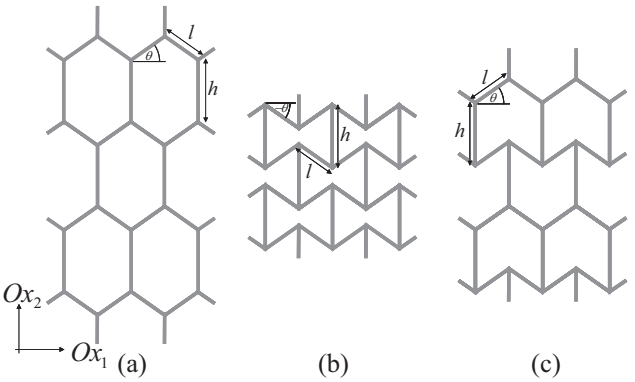

Figure 1 Geometry of the (a) conventional, (b) re-entrant honeycomb and (c) the semi re-entrant honeycomb.

the honeycombs deform through stretching, hinging and/or flexing. Nevertheless, the applicability of such hinging/flexing honeycombs for applications which require a zero Poisson's ratios is very limited as such behaviour is only exhibited in the limit of zero strain.

We have recently proposed a novel class of hexagonal honeycomb structures [76, 77] which, as illustrated in Fig. 1c, are constructed in such a way that their cells contain both re-entrant and non re-entrant features thus henceforth referred to as the 'semi re-entrant' honeycombs. Such honeycombs, which deform through flexure of the cell walls, have already been shown to exhibit two extremely useful mechanical properties namely (1) zero Poisson's ratio for loading in the Ox_1 direction for large strains; and (2) a high Young's modulus for loading in the Ox_2 direction, the latter property being in accordance with the predictions made by Lim [78] and Kocer et al. [79] for composites made from alternate layers of auxetic and conventional materials.

Nevertheless, as already explained by Evans et al. [3, 4], it is important to note that, although flexure may be the predominant deformation mechanism [3], it cannot be assumed that this mechanism acts alone. In fact, it is important to also consider additional modes of deformations which include stretching and hinging, all of which will in practice contribute to the overall deformation mechanism [3, 4].

In view of all this, in this work we extend our earlier work by deriving separate analytical models for the Young's moduli and Poisson's ratios for infinite planar networks of semi re-entrant honeycombs deforming through stretching (idealized stretching model) and hinging (idealized hinging model), two deformation mechanisms which may accompany flexure. This will be followed by an additional model which takes into account these three deformation mechanisms acting concurrently.

2 Idealized single mode models The derivations presented here for the idealized single mode models (idealized stretching, idealized hinging and idealized flexure) are based on the unit cell for a semi re-entrant

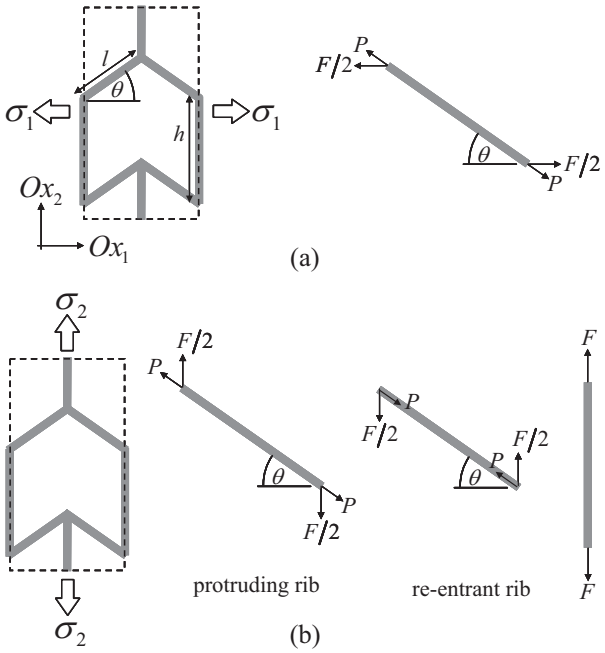

Figure 2 Force components acting along the inclined ribs when the semi re-entrant honeycomb deforms through stretching for loading in the (a) Ox_1 and (b) Ox_2 direction.

honeycomb shown in Fig. 2, where h and l are the lengths of the vertical and inclined ribs respectively and t is their thickness. This unit cell is oriented such that the vertical ribs are aligned along the Ox_2 direction as shown in Fig. 2 so that the projections of the unit cell in the Ox_1 and Ox_2 directions are respectively given by

$$X_1 = 2l\cos(\theta), \tag{1}$$

$$X_2 = 2h \tag{2}$$

It shall also be assumed that the thickness in the third direction is equal to z.

2.1 Idealized stretching model In this derivation it shall be assumed that the ribs have an associated stiffness constant ${K_s}^i$ where $i = h, l$ indicates the identity of the rib. Assuming that the material making up the honeycomb is isotropic and perfectly elastic, then by applying Hooke's law, the extension of each inclined rib as a result of an external load can be found since, the extension along the rib is given by $\delta = P/{K_s}^i$ where $P = F\cos(\theta)/2$ is the force acting parallel to the rib and F is the force in the Ox_i direction due to a stress σ_i related by $\sigma_i = F_i/A_i$ where A_i is the area over which the stress is acting. When such a structure is loaded in the Ox_1direction, only the inclined ribs deform and the corresponding extension δ_i is given by

$$\delta_l = \frac{F\cos(\theta)}{2{K_s}^l}. \tag{3}$$

Thus, the change in the projection of the unit cell X_1 in the Ox_1 direction is given by

$$\mathrm{d}X_1 = 2\delta_l \cos(\theta) = \frac{F_1 \cos^2(\theta)}{K_s^l}, \tag{4}$$

and therefore, the strain along this direction is given by

$$\varepsilon_1 = \frac{\mathrm{d}X_1}{X_1} = \frac{F_1 \cos(\theta)}{2K_s{}^l l} = \frac{hz\cos(\theta)}{K_s{}^l l}\sigma_1. \tag{5}$$

Since X_2 is only dependent on h (which in this case remains unchanged during loading), it follows that the component of the extension of the inclined ribs in the Ox_2 direction plays no role in changing the unit cell dimension in this direction. Thus the strain in the Ox_2 direction is

$$\varepsilon_2 = 0, \tag{6}$$

from which it follows that the Poisson's ratio is also zero since

$$\nu_{12} = -\frac{\varepsilon_2}{\varepsilon_1} = 0. \tag{7}$$

The Young's modulus $E_1^s = \sigma_1/\varepsilon_1$ can also be found by substituting for ε_1 using Eq. (5) as follows

$$E_1^s = \frac{K_s{}^l l}{zh\cos(\theta)}. \tag{8}$$

For loading in tension in the Ox_2direction, it is clearly evident from Fig. 2b that the re-entrant ribs are under compression and thus would be expected to contract in length whilst the protruding ribs are under tension thus would be expected to extend. (The opposite will happen for loading in compression.) Now, since we are assuming that the network is infinite and planar, edge effects cannot occur and therefore, it is not possible for the vertical ribs to tilt in such a way so as to accommodate such deformations. Consequently, deformation of the inclined ribs is resisted and only extensions in the vertical ribs are allowed. Thus, one may immediately note that since X_1 is independent of h, it remains unchanged so that for loading in the Ox_2 direction, $\varepsilon_1 = 0$ and as a result, the Poisson's ratio ν_{21} is also zero.

The extension along the vertical rib is simply given by

$$\delta_h = \frac{F_2}{K_s^h}, \tag{9}$$

where K_s^l and K_s^h are related by $K_s^h = K_s{}^l l/h$ and thus the strain along the Ox_1 direction is given by

$$\varepsilon_2 = \frac{\delta_h}{h} = \frac{F_2}{K_s^h h} = \frac{2zl\cos(\theta)}{K_s^h h}\sigma_2, \tag{10}$$

and the Young's modulus by

$$E_2^s = \frac{\sigma_2}{\varepsilon_2} = \frac{K_s^h h}{2lz\cos(\theta)}. \tag{11}$$

Note that the expressions for the moduli for the idealized stretching models involve stretching stiffness constants which are dependent on the lengths of the ribs *i.e.* the stiffness constant K_s^h used for the vertical ribs of length h are different from the slanting ribs of length l. This is justified since in real systems where the honeycombs are constructed from ligaments welded together at the joints, these stiffness constants would be given by

$$K_s^l = \frac{E_s t z}{l} \text{ and } K_s^h = \frac{E_s t z}{h}, \tag{12}$$

where E_s is the Young's modulus of the material making up the honeycomb, t the thickness of the rib and z is the depth of the rib in the Ox_3 direction.

However, it is also possible to re-write the expressions for the Young's moduli in terms of a single stretching force constant, for example $K_s{}^l$. In analogy to earlier work by Evans et al. [3, 4], under such assumption, the Young's modulus E_2 may be re-written as

$$E_2^s = \frac{K_s^l}{2z\cos(\theta)}. \tag{13}$$

It is important to note that the stretching model derived here is only applicable for tensile loading or for compressions if very small strains are used. At larger strains, the ribs become prone to buckling when the honeycomb is compressed, an effect which is not considered here.

2.2 Idealized hinging model Similar to the idealized stretching model, for loading in the Ox_2 direction, the inclined ribs cannot hinge since the re-entrant layer tend to open up the structure while the conventional layer ones tend to close it. Thus for the idealized hinging model representing an infinity large honeycomb, the structure is undeformable for loading in the Ox_2 direction so that the corresponding analytical model cannot be derived.

For loading in the Ox_1 direction, an infinitesimal change $\mathrm{d}\theta$ in the angle θ, the strain in the Ox_i direction can be expressed as

$$\varepsilon_i = \frac{1}{X_i}\left(\frac{\partial X_i}{\partial \theta}\right)\mathrm{d}\theta. \tag{14}$$

Thus from Eq. (1) and Eq. (2), it follows that

$$\varepsilon_1 = -\tan(\theta)\mathrm{d}\theta, \tag{15}$$

$$\varepsilon_2 = 0. \tag{16}$$

Thus the Poisson's ratio for loading in the Ox_1 direction is given by

$$\nu_{12} = -\frac{\varepsilon_2}{\varepsilon_1} = 0. \tag{17}$$

The Young's modulus can be found using an energy approach. Each of the joints can effectively be replaced by two hinges as shown in Fig. 3 so that each rib is connected to

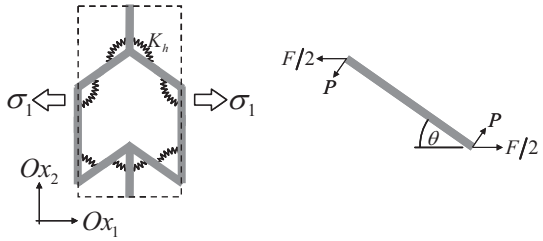

Figure 3 Force components acting perpendicular to the inclined ribs when the semi re-entrant honeycomb deforms through hinging when loading in the Ox_1.

adjacent ribs through such hinges. Then in each unit cell, which contains four joints, there are eight hinges. Assuming that all the work done in deforming the structure is stored as strain energy in these hinges then, the energy stored per unit volume is given by

$$U = \frac{1}{2} E_i^h \varepsilon_i^2, \tag{18}$$

where E_i^h is the Young's modulus of the structure which deforms only through hinging for loading in the Ox_i direction and U is related to the work done w at each hinge through

$$U = \frac{n}{V} w, \tag{19}$$

where n is the number of hinges in the unit cell, V the volume of the unit cell given by $V_1 = X_1 X_2 z$ and $w = k_h (\mathrm{d}\theta)^2/2$. Thus, in this case, assuming thickness z in the third direction

$$U = \frac{2k_h (\mathrm{d}\theta)^2}{2zhl\cos(\theta)} = \frac{1}{2} E_i^h \varepsilon_i^2, \tag{20}$$

and substituting for ε_i using Eq. (15), the Young's modulus for loading in the Ox_1 direction is given by

$$E_1^h = \frac{2k_h \cos(\theta)}{zhl \sin^2(\theta)}. \tag{21}$$

Note that in analogy to the work by Evans et al., the k_h due to the stiffness of two hinges connected to each slanting rib may be replaced by a K_h which defines the resistance of this rib to rotate by an angle $\mathrm{d}\theta$ where clearly $K_h = 2k_h$. In such case, the expression for the Young's modulus for the idealized hinging model may be re-written as

$$E_1^h = \frac{K_h \cos(\theta)}{zhl \sin^2(\theta)}. \tag{22}$$

2.3 Idealized flexure model The analytical model that describes the flexural behaviour of these types of honeycombs has already been derived in Refs. [76, 77]. In particular, it was shown that the Poisson's ratio and Young's modulus for a honeycomb deforming solely through flexure when stretched in the Ox_1 direction are respectively given by

$$\nu_{12} = -\frac{\varepsilon_2}{\varepsilon_1} = 0, \tag{23}$$

$$E_1^{\mathrm{f}} = \frac{\sigma_1}{\varepsilon_1} = \left(\frac{t}{l}\right)^3 \left(\frac{l}{h}\right) \frac{E_{\mathrm{s}} \cos(\theta)}{\sin^2(\theta)}, \tag{24}$$

where θ, l and h are as defined in Fig. 2 and E_{s} is the Young's modulus of the material.

Note that in analogy to earlier work, this expression for the Young's modulus may be re-written in terms of a flexure stiffness constant, K_{f} as

$$E_1^{\mathrm{f}} = \frac{K_{\mathrm{f}} \cos(\theta)}{zhl \sin^2(\theta)}, \tag{25}$$

where K_{f} is defined by [3, 4]

$$K_{\mathrm{f}} = \frac{E_{\mathrm{s}} z t^3}{l}. \tag{26}$$

Note that Eq. (25) for the Young's modulus for the idealized flexure model is of the same format as that of Eq. (22) for the Young's modulus of the idealized hinging model, something which may be expected and is concordant with earlier work on conventional and re-entrant honeycombs [3, 4].

Also, once again, as in the idealized hinging model, one should note that the mechanical properties of idealized infinitely large systems for loading in the Ox_2 directions cannot be derived as such systems would have an infinite modulus in this direction if the systems deforms solely through flexure (idealized flexing model).

3 Combined flexure/hinging/stretching model

The properties of a system which deform solely through 'flexure', 'hinging' or 'stretching' presented above are highly idealized scenarios, as in reality, one would expect that there is some superposition of effects given by flexure, stretching and hinging of the ribs. For systems where the material is linearly elastic and assuming that only small deformations occur, then, for loading by a stress σ_i in an Ox_i ($i = 1, 2$) direction, the strains in the Ox_i direction are given by

$$\varepsilon_i^{\mathrm{s+h+f}} = \varepsilon_i^{\mathrm{s}} + \varepsilon_i^{\mathrm{h}} + \varepsilon_i^{\mathrm{f}}, \tag{27}$$

where $\varepsilon_i^{\mathrm{s}}$ is the strain due to stretching, $\varepsilon_i^{\mathrm{h}}$ the strain due to hinging and $\varepsilon_i^{\mathrm{f}}$ is the strain due to flexing. But since a strain ε_i in an Ox_i direction is related to a stress σ_i in the same direction through

$$\varepsilon_i = \frac{1}{E_i} \sigma_i, \tag{28}$$

where E_i is the Young's modulus in the Ox_i direction, then from Eqs. (27) and (28)

$$\frac{\sigma_i}{E_i^{\mathrm{s+h+f}}} = \frac{\sigma_i}{E_i^{\mathrm{s}}} + \frac{\sigma_i}{E_i^{\mathrm{h}}} + \frac{\sigma_i}{E_i^{\mathrm{f}}}, \tag{29}$$

where E_i^{s+h+f} is the Young's modulus in the Ox_i direction due to concurrent stretching, hinging and flexing, E_i^s, E_i^h and E_i^f are the Young's modulus in the Ox_i direction due to stretching, hinging and flexing, respectively.

By rearranging Eq. (29), and substituting for E_i^s, E_i^h and E_i^f using Eqs. (8), (22) and (25), respectively, the Young's modulus for loading in an Ox_i direction ($i = 1, 2$) for systems deforming through concurrent stretching, hinging and flexing is therefore given by

$$E_i^{s+h+f} = \frac{E_i^s E_i^h E_i^f}{E_i^h E_i^f + E_i^s E_i^f + E_i^s E_i^h}, \tag{30}$$

so that for loading in the Ox_1 direction the Young's modulus is given by

$$E_1^{s+h+f} = \frac{K_s{}^l K_h K_f \cos(\theta)}{zhl \sin^2(\theta)\left[\dfrac{K_h K_f}{l^2 \tan^2(\theta)} + K_s{}^l K_f + K_s{}^l K_h\right]}. \tag{31}$$

Furthermore, since from Eq. (7) the strain in the orthogonal Ox_j direction are given by

$$\varepsilon_j = -\nu_{ji}\varepsilon_i = \frac{-\nu_{ji}}{E_i}\sigma_i, \tag{32}$$

and since in analogy to Eq. (27)

$$\varepsilon_j^{s+h+f} = \varepsilon_j^s + \varepsilon_j^h + \varepsilon_j^f, \tag{33}$$

then from Eq. (32) and Eq. (33)

$$\frac{-\nu_{ij}^{s+h+f}\sigma_i}{E_i^{s+h+f}} = \frac{-\nu_{ij}^s\sigma_i}{E_i^s} + \frac{-\nu_{ij}^h\sigma_i}{E_i^h}\frac{-\nu_{ij}^f\sigma_i}{E_i^f}, \tag{34}$$

where ν_{ij}^{s+h+f} is the Poisson's ratio in the Ox_i–Ox_j plane for loading in the Ox_i direction due to concurrent stretching, hinging and flexing, ν_{ij}^s, ν_{ij}^h and ν_{ij}^f are the Poisson's ratio in the Ox_j–Ox_j plane for loading in the Ox_i direction due to stretching, hinging and flexing, respectively, all of which have a null value so that the Poisson's ratio for the concurrent model is also zero.

4 Discussion The idealized models in Section 2 above present expressions for the mechanical properties of idealized models involving solely hinging at the joints, flexure of the ligaments or stretching of the ligaments. Such models can be particularly useful in a theoretical investigation as they shed light on the potential of each mechanism to generate the required property, in this case zero Poisson's ratio. Also, in some cases, a single mode model may be sufficient to describe the property of a realistic system. A practical example of this are honeycombs constructed from cardboard which tend to deform through hinging as a result of the weakness that is introduced at the joints when folding the cardboard (see Fig. 4). Nevertheless, in general, it should be noted that it is usual for a mechanism to be accompanied by other mechanisms and that in reality a model which can capture more than one deformation mechanism would be desirable since, in general, it offers a better representation of real systems.

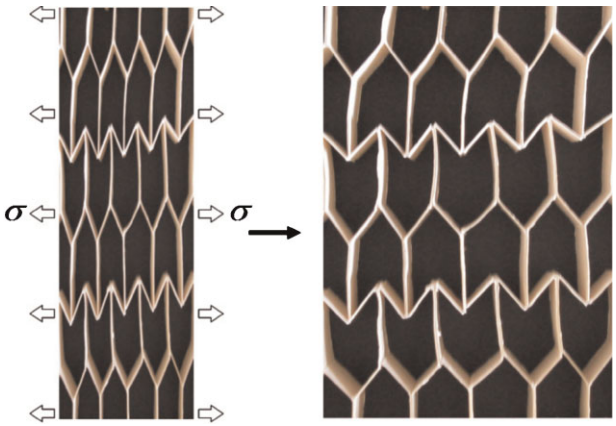

Figure 4 (online colour at: www.pss-b.com) Deformation in a semi re-entrant honeycomb made of cardboard, showing that in such a honeycomb deformation occurs mainly through hinging.

For example, in macro/micro structured honeycombs, stretching and flexing are usually not independent of each other since both are dependent on the Young's modulus of the material. Thus, for example a low Young's modulus would make the ribs not only easier to flex but also easier to stretch. The relative magnitude of these deformation mechanisms depends on various factors namely the tilting angle, θ, of the rib, its thickness and also its length. In particular, it is possible to write an expression for the relative magnitude of the two mechanisms using Eqs. (8) and (25) as follows:

$$\frac{E_1{}^s}{E_1{}^f} = \frac{l^2 \tan(\theta)}{t^2}. \tag{35}$$

Thus, it is evident that a smaller angle favours stretching since the force component along the rib leading to stretching would be larger than the perpendicular one which results in flexing/hinging. Thus, for example, as illustrated in Fig. 5, at low θ-values, the Young's modulus due to flexure alone is so high that deformation occurs almost exclusively through stretching so that the Young's modulus of the honeycomb is almost equal to E^s.

It is also apparent that thin ribs favour flexing since the Young's modulus for flexure has a t^3 dependency whereas that of stretching has a t dependency. At small t values flexure dominates but as t increases, the ribs become increasingly difficult to flex at a much higher rate compared to stretching so that the latter starts to become more significant. However, for slender beams, this effect is almost negligible so unless the thickness is comparable to the length of the rib, flexure remains as the dominant mechanism as has been observed in Refs. [1, 2].

Also interesting to note is that only flexing/hinging are affected by changes in length. In particular an increase in

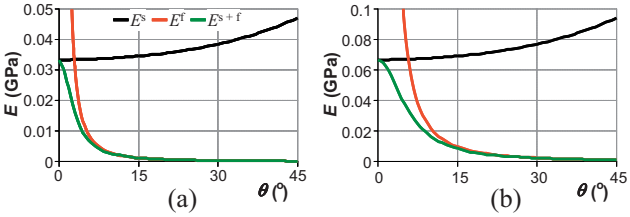

Figure 5 (online colour at: www.pss-b.com) Plots showing the variation of the Young's modulus for stretching, flexing and combined stretching and flexing as a function of θ. For these particular cases, $l = 10$, $h = 15$, $E_s = 1$ GPa and (a) $t = 0.5$, (b) $t = 1$.

l favours these mechanisms since the longer the rib is the larger the moment available to flex/hinge the rib. Thus, at relatively large l values, flexing hinging are the dominating mechanisms. It is important to note that the extent of hinging also depends on the way the system is constructed. Thus, if real hinges are used at the joints, then hinging does not depend on the material used but only on the force constant of the hinges. However, if the honeycomb does not have such hinges and instead is entirely made of the same material, then it will also depend on the mechanical properties of the material used. All this suggests that for a correct treatment of the mechanical properties it is important that all three deformation mechanisms are taken into consideration.

Nevertheless, it is important to note that for this particular honeycomb, the mode of deformations makes no difference on the main required property, that of a zero Poisson's ratio since the combined mechanisms would exhibit this property irrespective of which of the three mechanisms discussed here (*i.e.* flexing, stretching and/or hinging) operates. In such cases, deviations from this property are more likely to arise as a result of defects in the geometry, in analogy with the work on similar hexagonal conventional and re-entrant honeycombs [80, 81]. For example it should be emphasized that if some of the ribs in the honeycomb are broken, then the required property of zero Poisson's ratio may not be manifested since in such cases, the main deformations would be dictated by the type and extent of the defect.

It should also be noted that the property referred to above in the idealized hinging and/or flexure model in the Ox_2 direction, that is their undeformability, is a highly idealized scenario and would only have occurred in infinitely large systems. Real honeycombs, particularly macro honeycombs, are unlikely to be infinitely large and in such cases deformations for loading in the Ox_2 direction may be allowed by permitting end effects. For example, earlier work has shown that in the case of the idealized flexure model, deformation of each individual cell is different from that of adjacent ones and is highly dependent on its position within the network, where the closer to the edge parallel to the Ox_2direction, the larger the deformation [77, 82]. Furthermore, despite these types of deformations (not accounted by the model presented here), it has been shown that the networks still exhibit a very large Young's modulus compared to both conventional and re-entrant honeycombs. Similar effects are also expected for the idealized hinging model.

Another interesting feature of the model presented here is its scale independency *i.e.* irrespective of the dimensions of the honeycomb, the Poisson's ratio is always zero. This makes it possible to manifest this effect not only at a macrolevel but also at any length scale including the microlevel (*e.g.* in foams) and nanolevel (*i.e.* in molecular networks) if similar geometric features and deformation mechanisms as described here are present. Materials with a zero Poisson's ratio are not very common (such materials include cork [83], membrane in beetle's wings [84] and polymer gels [85]) and very often this effect is achieved by using composite materials that are specifically engineered to exhibit such property. However such composites may suffer from failure at the interface and therefore there is the need to produce alternative zero Poisson's ratio materials which do not suffer from these problems.

Before we conclude it is important to highlight some of the advantages of the honeycombs presented here as opposed to conventional and/or auxetic honeycombs. Apart from being useful in applications where changes in lateral dimensions caused by loading are undesired, these honeycombs also have a natural ability to be morphed into a tubular structure. This is not possible with conventional and auxetic honeycombs since their tendency to form saddle and dome shaped surface respectively causes stresses in the honeycomb were they to be morphed into cylindrical structures. The main reason for such behaviour is that downward bending of a conventional honeycomb in one direction puts its upper surface under tension along the direction of bending so that in the transverse direction the upper surface contracts and curves upwards to adopt the saddle shaped configuration (see Fig. 6a). Conversely, in auxetic honeycombs, downward bending (*i.e.* extension) in one direction is accompanied by an expansion in the lateral direction forcing the honeycomb to also bend downward in this direction and hence adopt a dome shaped configuration (see Fig. 6b). However, in semi re-entrant honeycombs, the lateral direction remains unaffected by bending enabling them to form a cylindrical surface (see Fig. 6c). Such a feature may be very useful for honeycomb cores in sandwich composites used in applications where the sandwich is morphed into a tubular structure and also in biomedical applications.

5 Conclusion This paper has shown that infinite and planar sheets of honeycombs with a semi re-entrant geometry exhibit the relatively rare property of a zero Poisson's ratio irrespective of the relative magnitude of the stretching, hinging and flexing mechanism or which of these deformation mechanism(s) is present. We hope that this work serves as a stimulus to researchers in designing similar systems with the ability to exhibit zero Poisson's ratio and also look forward to their implementation on a micro and nano level to synthesize new materials with this property that

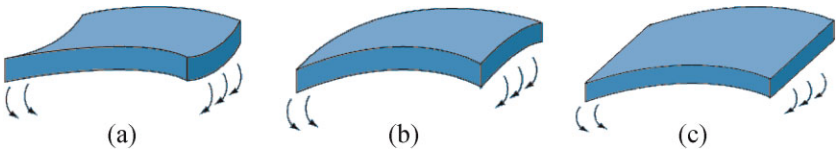

Figure 6 (online colour at: www.pss-b.com) Bending in (a) conventional, (b) auxetic and (c) zero Poisson's ratio material. The edges along which the bending stress is applied deform in a different manner in each case. In conventional materials the edge curves upward to form a saddle shape (a), in auxetic materials it curves downwards to form a dome shape (b) while in zero Poisson's ratio materials it remains straight (c).

could be used as an alternative to naturally occurring materials like cork.

Acknowledgements This work is supported by the Government of Malta through an MGSS grant awarded to Daphne Attard. The very useful discussions with Dr. Ing. Ludovica Oliveri from the University of Catania during her stay at the University of Malta are also gratefully acknowledged.

References

[1] L. J. Gibson, M. F. Ashby, G. S. Schajer, and C. I. Robertson, Proc. R. Soc. London A **382**, 25 (1982).
[2] L. J. Gibson and M. F. Ashby, Cellular Solids Structure and Properties, 2nd ed. (Cambridge University Press, UK, 1997).
[3] I. G. Masters and K. E. Evans, Compos. Struct. **35**, 401 (1996).
[4] K. E. Evans, A. Alderson, and F. R. Christian, J. Chem. Soc. Faraday Trans. **91**, 2671 (1995).
[5] H. X. Zhu and N. J. Mills, Int. J. Solids Struct. **37**, 1931 (2000).
[6] E. Wu and W. S. Jiang, Int. J. Impact Eng. **19**, 439 (1997).
[7] T. Wierzbicki, Int. J. Impact Eng. **1**, 157 (1983).
[8] S. D. Papka and S. Kyriakides, Acta Mater. **46**, 2765 (1998).
[9] S. D. Papka and S. Kyriakides, Int. J. Solids Struct. **36**, 4367 (1999).
[10] S. D. Papka and S. Kyriakides, Int. J. Solids Struct. **36**, 4397 (1999).
[11] F. Scarpa and P. J. Tomlin, Fatigue Fract. Eng. Mater. Struct. **23**, 717 (2000).
[12] F. C. Smith, F. Scarpa, and B. Chambers, IEEE Microwave Guided Wave Lett. **10**, 451 (2000).
[13] M. Ruzzene, L. Mazzarella, T. Panagiotis, and F. Scarpa, J. Intel. Mater. Syst. Struct. **13**, 587 (2002) (application).
[14] M. J. Silva, L. J. Gibson, and W. C. Hayes, Int. J. Mech. Sci. **37**, 1161 (1995).
[15] M. A. Fortes and M. F. Ashby, Acta Mater. **47**, 3469 (1999).
[16] R. Lakes, J. Mater. Sci. **26**, 2287 (1991).
[17] D. Prall and R. S. Lakes, Int. J. Mech. Sci. **39**, 305 (1997).
[18] J. Martin, J. J. Heyder-Bruckner, C. Remillat, F. Scarpa, K. Potter, and M. Ruzzene, Phys. Status Solidi B **245**, 570 (2008).
[19] F. Scarpa, S. Blain, T. Lew, D. Perrott, M. Ruzzene, and J. R. Yates, Composites A **38**, 280 (2007).
[20] J. N. Grima, R. Gatt, and P. S. Farrugia, Phys. Status Solidi B **245**, 511 (2008).
[21] A. Alderson, K. L. Alderson, D. Attard, K. E. Evans, R. Gatt, J. N. Grima, W. Miller, N. Ravirala, C. W. Smith, and K. Zied, Compos. Sci. Technol., doi:10.1016/j.compscitech.2009.07.009.
[22] N. Gaspar, X. J. Ren, C. W. Smith, J. N. Grima, and K. E. Evans, Acta Mater. **53**, 2439 (2005).
[23] C. W. Smith, J. N. Grima, and K. E. Evans, Acta Mater. **48**, 4349 (2000).
[24] M. A. Nkansah, K. E. Evans, and I. J. Hutchinson, Modell. Simul. Mater. Sci. Eng. **2**, 337 (1994).
[25] F. Scarpa, P. Panayiotou, and G. Tomlinson, J. Strain Anal. **35**, 383 (2000).
[26] A. Bezazi, F. Scarpa, and C. Remillat, Compos. Struct. **71**, 356 (2005).
[27] J. P. M. Whitty, A. Alderson, P. Myler, and B. Kandola, Composites A **34**, 525 (2003).
[28] R. F. Almgren, J. Elast. **15**, 427 (1985).
[29] U. D. Larsen, O. Sigmund, and S. Bouwstra, MEMS'96 Proceedings, 1996, p. 365.
[30] J. N. Grima, R. Gatt, A. Alderson, and K. E. Evans, Mol. Simul. **31**, 925 (2005).
[31] H. Tanaka and Y. Shibutani, J. Mech. Phys. Solids **57**, 1485 (2009).
[32] J. B. Choi, and R. S. Lakes, Int. J. Mech. Sci. **37**, 51 (1995).
[33] K. E. Evans, M. A. Nkansah, and I. J. Hutchinson, Acta Metall. Mater. **42**, 1289 (1994).
[34] K. E. Evans, M. A. Nkansah, I. J. Hutchinson, and S. C. Rogers, Nature **353**, 124 (1991).
[35] R. Lakes, Science **235**, 1038 (1987) (application).
[36] C. B. He, P. W. Liu, P. K. McMullan, and A. C. Griffin, Phys. Status Solidi B **242**, 576 (2005).
[37] C. B. He, P. W. Liu, and A. C. Griffin, Macromolecules **31**, 3145 (1998).
[38] R. H. Baughman and D. S. Galvao, Nature **365**, 735 (1993).
[39] A. Alderson, P. J. Davies, M. R. Williams, K. E. Evans, K. L. Alderson, and J. N. Grima, Mol. Simul. **31**, 897 (2005).
[40] J. N. Grima and K. E. Evans, Chem. Commun. **16**, 1531 (2000).
[41] J. N. Grima, D. Attard, R. N. Cassar, L. Farrugia, L. Trapani, and R. Gatt, Mol. Simul. **34**, 1149 (2008).
[42] J. N. Grima, A. Alderson, and K. E. Evans, J. Phys. Soc. Jpn. **74**, 1341 (2005).
[43] R. S. Lakes and K. Elms, J. Compos. Mater. **27**, 1193 (1993) (application).
[44] N. Chan and K. E. Evans, J. Cell Plast. **34**, 231 (1998) (application).
[45] K. L. Alderson and K. E. Evans, J. Mater. Sci. **28**, 4092 (1993).
[46] K. E. Evans and B. D. Caddock, J. Phys. D: Appl. Phys. **22**, 1883 (1989).
[47] A. Alderson and K. E. Evans, J. Mater. Sci. **32**, 2797 (1997).
[48] R. H. Baughman, J. M. Shacklette, A. A. Zakhidov, and S. Stafstrom, Nature **392**, 362 (1998).

[49] A. Yeganeh-Haeri, D. J. Weidner, and J. B. Parise, Science **257**, 650 (1992).
[50] N. R. Keskar and J. R. Chelikowsky, Nature **358**, 222 (1992).
[51] A. Alderson, K. L. Alderson, K. E. Evans, J. N. Grima, M. R. Willams, and P. J. Davies, Phys. Status Solidi B **242**, 499 (2005).
[52] J. N. Grima, R. Gatt, A. Alderson, and K. E. Evans, J. Mater. Chem. **15**, 4003 (2005).
[53] H. Kimizuka, S. Ogata, and Y. Shibutani, Phys. Status Solidi B **244**, 900 (2007).
[54] A. Alderson and K. E. Evans, Phys. Rev. Lett. **89**, 225503 (2002).
[55] J. N. Grima, R. Jackson, A. Alderson, and K. E. Evans, Adv. Mater. **12**, 1912 (2000).
[56] J. N. Grima, V. Zammit, R. Gatt, A. Alderson, and K. E. Evans, Phys. Status Solidi B **244**, 866 (2007).
[57] J. N. Grima, R. Gatt, V. Zammit, J. J. Williams, K. E. Evans, A. Alderson, and R. I. Walton, J. Appl. Phys. **101**, 086102 (2007).
[58] J. J. Williams, C. W. Smith, K. E. Evans, Z. A. D. Lethbridge, and R. I. Walton, Chem. Mater. **19**, 2423 (2007).
[59] C. Sanchez-Valle, S. V. Sinogeikin, Z. A. D. Lethbridge, R. I. Walton, C. W. Smith, K. E. Evans, and J. D. Bass, J. Appl. Phys. **98**, 053508 (2005).
[60] K. W. Wojciechowski, Phys. Lett. A **137**, 60 (1989).
[61] K. W. Wojciechowski and A. C. Branka, Phys. Rev. A **40**, 7222 (1989).
[62] C. Remillat, F. Scarpa, and K. W. Wojciechowski, Phys. Status Solidi B **246**, 2007 (2009).
[63] J. N. Grima and K. W. Wojciechowski, Phys. Status Solidi B **245**, 2369 (2008).
[64] C. W. Smith and K. W. Wojciechowski, Phys. Status Solidi B **245**, 486 (2008).
[65] K. W. Wojciechowski, A. Alderson, K. L. Alderson, B. Maruszewski, and F. Scarpa, Phys. Status Solidi B **244**, 813 (2007).
[66] K. W. Wojciechowski, A. Alderson, A. Braka, and K. L. Alderson, Phys. Status Solidi B **242**, 497 (2005).
[67] F. Scarpa, L. G. Ciffo, and J. R. Yates, Smart Mater. Struct. **13**, 49 (2004).
[68] C. W. Smith, F. Lehman, R. J. Wootton, and K. E. Evans, Cell Polym. **18**, 79 (1999).
[69] J. B. Choi and R. S. Lakes, Cell Polym. **10**, 205 (1991).
[70] R. E. Moyers, US Patent No. 5108413, 1992.
[71] B. D. Caddock and K. E. Evans, Biomaterials **16**, 1109 (1995).
[72] K. E. Evans, Endeavour **15**, 170 (1991).
[73] M. Burke, New Sci. **154**, 36 (1997).
[74] K. E. Evans and A. Alderson, Eng. Sci. Educa. J. 148 (2000).
[75] C. P. Chen and R. S. Lakes, Cell Polym. **8**, 343 (1989).
[76] J. N. Grima, L. Oliveri, D. Attard, R. Gatt, B. Ellul, G. Cicala, and G. Recca, 6th Int. Workshop on Auxetics and Related Systems, Bolton, UK, 2009.
[77] J. N. Grima, L. Oliveri, D. Attard, B. Ellul, R. Gatt, G. Cicala, and G. Recca, Adv. Eng. Mater., in press.
[78] T. C. Lim, Eur. J. Mech. A **28**, 752 (2009).
[79] C. Kocer, D. R. McKenzie, and M. M. Bilek, Mater. Sci. Eng. A **505**, 111 (2009).
[80] E. J. Horrigan, C. W. Smith, F. L. Scarpa, N. Gaspar, A. A. Javadi, M. A. Berger, and K. E. Evans, Mech. Mater. **41**, 919 (2009).
[81] B. Ellul, R. Gatt, D. Attard, and J. N. Grima, On the effect of disorder on the Poisson's ratios of hexagonal honeycombs, paper presented at 5th International Conference Physics of Disordered Systems '10, 23–27 May 2010, Gdansk-Sobieszewo, Poland.
[82] L. Oliveri, PhD Thesis, University of Catania, Italy, 2009.
[83] L. J. Gibson, K. E. Easterling, and M. F. Ashby, Proc. R. Soc. London A **377**, 99 (1981).
[84] T. Jin, N. S. Goo, S. C. Woo, and H. C. Park, J. Bionic Eng. **6**, 224 (2009).
[85] E. Geissler and A. M. Hecht, Macromolecules **13**, 1276 (1980).